Angewandte Chemie
Eine Zeitschrift der Gesellschaft Deutscher Chemiker

Supporting Information

Fuel-Driven and Enzyme-Regulated Redox-Responsive Supramolecular Hydrogels

*Mehak Jain and Bart Jan Ravoo**

anie_202107917_sm_miscellaneous_information.pdf

Supporting Information

Table of Contents

Materials and Methods

(i) Materials

Polyacrylic acid (Mw 450 kDa, 181285, pAA), peroxidase (from Horseradish, lyophilized powder, ≥ 139 units mg^{-1}, 73292, HRP) glucose oxidase (from Aspergillus Niger, lyophilized powder, ≥ 100 units mg^{-1}, 61788, GOx) were purchased from Sigma Aldrich. Benzotriazol-1-yl-oxytripyrrolidinophosphonium hexafluorophosphate (PyBOP, Carbolution), beta-cyclodextrin (β-CD,Wacker), ferrocene carboxylic acid (FcCOOH, Abcr chemicals), ferrocene acetic acid (Fc, TCI chemicals) ethylenediamine (EDA, Acros Organics), 1-(p- toluenesulfonyl)imidazole (Acros Organics), sodium azide (Acros Organics), triphenylphosphine (Flurochem), 1,1,2,2 tetrachloroethane (Acros Organics). Triethylamine (ET_3N, Acros Organics), D-glucose anhydrous (Fischer scientific), 30% peroxide solution (Fischer scientific). Snake skin dialysis tubing MWCO (10 kDa cut off, 35 mm dry ID, 88245) was bought from Thermo Scientific, USA. Boric acid, KCl pallets and NaOH pallets were purchased from Merck.

(ii) Gel formation

4 wt% solutions of pAA-CD and pAA-Fc were prepared in (0.1 M) boric acid-KCl buffer at pH 9.0. Mixing of both polymer solutions (host: guest) in (1:0.5), (1:1), (1.25:1), ratios gave the desired gel with varying storage modulus (G'). For all the experiments (1.25:1) (pAA-CD : pAA-Fc) with G' = 100Pa was used. These gels were stable for more than 30 d.

(iii) UV-vis spectroscopy

All measurements were carried out using JASCO V-770 spectrophotometer with Peltier support to allow continuous stirring and maintaining temperature at 25℃ for all the experiments. The samples were analyzed using high precision 3 mL SUPRASIL quartz

glass cuvettes with 1 cm path length. All the samples were baseline corrected prior to measuring absorbance against (0.1 M) sodium phosphate buffer pH 7.6.

(a) Redox properties of ferrocene acetic acid

2 mM Ferrocene acetic acid solution along with oxidation and reduction fuels were prepared in (0.1 M) sodium phosphate buffer pH 7.6. The enzymes used for oxidation and reduction of Fc were Horseradish Peroxidase (HRP) with substrate Peroxide (H_2O_2) (oxidation fuel) and Glucose Oxidase (GOx) with substrate D-Glucose (reduction fuel) respectively. To 3 mL Fc aqueous solution 0.1 mM of HRP and 3 mM of oxidation fuel was added and reaction mixture was stirred continuously. Absorption spectra at different time intervals was recorded with emergence of an oxidation peak at 630 nm. For reduction, to same oxidized Ferrecenium solution (Fc^+) 0.1 mM of GOx and 5 mM reduction fuel was added and absorption spectra was recorded with 630 nm absorption peak decreasing with time (Fig 1a).

(b) Re-oxidation of ferrocene acetic acid

Time dependent UV-vis analysis at 630 nm were carried out for understanding the re-oxidation behavior of Fc. 2mM Fc solution in pH 7.6 sodium phosphate buffer was oxidized using oxidation fuel (0.1 mM of HRP and 3 mM of H_2O_2) to give Fc^+ ions. For the analysis 3mL of above prepared Fc^+ ions solution was utilized with constant stirring at 1000 rpm. At t=0 min, 0.1 mM of GOx and 5 mM of D-glucose (reduction fuel) was added and measurement was started instantly. Absorbance was recorded continuously after every 2 min at 630 nm. The spectra showed an instant decrease of absorbance with gradual increase after nearly 60 min (Fig 1c).
Different concentrations of D-Glucose (1 mM to 20 mM) were used to understand the correlation with rate of re-oxidation. Each measurement was triplicated for confidence in values and the trend observed (Fig. S6). All samples were triplicated with constant reaction conditions.

(c) Michaelis-Menten kinetics

For understanding the key mechanism underlying the re-oxidation, Michaelis-Menten kinetics were studied to understand three major events:

(a) Oxidation of ferrocene to ferrocenium ion in the presence of HRP and H_2O_2:
Kinetics assay was performed between 0.1 mg mL^{-1} of HRP and increasing concentrations of Fc (substrate) ranging from 0.1 µM to 500 µM in the presence of dilute 1% H_2O_2. Typically, the reaction mixture comprised of 2 mL substrate, 10 µL 1% H_2O_2 and 100 µL HRP. Oxidation of ferrocene was measured at 25℃ continuously for 15 min with constant stirring and continuous product formation monitored at 630 nm (Fig. S3a).

(b) Reduction of ferrocenium ion to ferrocene in the presence of GOx and D-glucose:
Kinetic assay was performed between 0.1 mg mL^{-1} of GOx and different concentrations of ferrocenium ion (substrate) ranging from 0.1 µM to 500 µM in the presence D-glucose. The reaction mixture comprised of 1 mL of substrate, 1 mL (3.5 wt. /v %) D-glucose and 100 µL GOx. Reduction of ferrocenium ion was measured at 25℃ continuously for 15 min with constant stirring and monitored at 630 nm using UV visible spectrophotometer (Fig. S3b).

(c) Generation of H_2O_2 during reaction between GOx and D-glucose in the presence of oxygen:
Kinetic assay was performed between constant amount of HRP and GOx (0.1 $mgmL^{-1}$) and increasing concentrations of D-glucose ranging from 0.1 to 400 µM. ABTS as reporter chromophore was employed and a constant amount (0.150 mM) was added to each set of measurement. The reaction mixture comprised of 1 mL D-Glucose substrate, 1 mL ABTS, 100 µL HRP and 100 µL GOx. Formation of $ABTS^{\bullet+}$ was measured at 25℃ continuously for 15 min with constant stirring and monitored at 410 nm using UV visible spectrophotometer (Fig. S3c).

Michaelis-Menten fitting (using Origin software function) was used to calculate various parameters for enzyme kinetics *viz.* V_{max} (maximum initial velocity), K_M (Michaelis-Menten constant), k_{cat} (turnover number) and k_{cat}/K_M (catalytic efficiency). All measurements were triplicated with constant reactions conditions.

(d) Supramolecular gel as D-glucose sensor

To test sensitivity of hydrogel towards D-Glucose, UV-vis experiments were performed in the presence and absence of D-Glucose. Samples for both control and D-glucose sensing hydrogel were prepared by addition of 0.3 mM of HRP and GOx along with 0. 8 mM carboxyfluorescein dye to the polymer solution while making the hydrogel. Both hydrogels were packed in a small dialysis tubing (MWCO 1 kDa) with both ends sealed. While the sample hydrogel was immersed in a 0.6 M glucose solution, the control hydrogel had only sodium phosphate buffer solution outside. Amount of dye released was tested using UV-vis spectroscopy over a period of 5 h by drawing 2mL sample from the bulk solution (Fig. S13).

(iv) Rheology measurements

All the rheological measurements were carried out using Anton Paar Modular Compact Rheometer MCR 102 with Anton Paar Rheo Compass V1.20.40.496 analysis software. In all measurements the gels were sandwiched between base and a cone plate CP25-2 (Anton Paar) spindle (25 mm diameter, 2 degree angle) at constant temperature 25℃.

(a) Linear viscoelastic region and self-healing behavior

Amplitude sweeps were carried out by transferring 0.25 µL of gel on to the rheometer cell and sandwiching against the CP25-2 cone plate spindle by maintaining a minimum distance of 0.106 mm. The measurement was carried out at fixed angular frequency ω=1.0 rad/sec while changing the sheer strain from 0.1% to 10%. For analyzing the linear viscoelastic region G' and G" were plotted against the deformation (Fig. S7).

Time dependent thixotropy measurements were performed on hydrogel at constant angular frequency 1.0 rad/sec by changing the sheer strain from 0.1 % to 1000 % in a consecutive order for fixed time period of 100 s after which γ resumed to 0.1% at the end of the measurement. The hydrogel showed pseudo-plastic behavior at higher γ rates and recovered back to its original storage moduli after decreasing sheer strain to 0.1% (Fig. S8) depicting self-healing properties.

(b) Oxidation

Samples were prepared by addition of (0.3 mM or 0.5 mM HRP and constant 0.25 M of H_2O_2) oxidation fuel to 400 µL hydrogel led by gentle stirring at 100 rpm for 5 min at room temperature to allow homogenous mixing of fuel. After which nearly 250 µL of hydrogel sample was transferred on to the rheometer cell. Time dependent gel to sol transformation was analyzed by measuring changes in storage modulus and loss modulus after constant intervals of 20 min at constant γ=1 % and ω=1 rad/sec until the gel changed to sol (Fig S9).

(c) Reduction

Samples for reassembly of gel were prepared by taking 400 µL of fresh sol (containing HRP (0.3 mM) from oxidation) adding constant amount of GOx (0.3 mM) and varying the concentration of solid D-Glucose (0.054 M to 0.96 M). Each sample was gently stirred at 100 rpm for 5 mins at room temperature before transferring to the rheometer. Time dependent sol to gel transformation was analyzed by measuring changes in G' and G" after constant intervals of 30 mins at constant γ=1 % and ω=1 rad/sec for ~900 mins. All samples were triplicated with constant reaction conditions.

(d) Glucose sensor

Self-regulating behavior of hydrogel was tested in the absence of hydrogen peroxide. Samples were prepared by addition of 0.3 M HRP and GOx to the hydrogel led by gentle stirring for 5 mins. After which 0.66 M D-Glucose was added to the hydrogel and a part of which was transferred to the rheometer. Continuous time dependent measurements for G' and G" were carried out at regular intervals of 30 min. After a successful cycle of transformation from gel-sol, the part of sol was refueled with 0.66 M of D-Glucose to run another cycle of sol-gel-sol transitions. All measurements were duplicated with constant reaction conditions.

(v) Control experiments

(i) Control experiment to determine presence of excess H_2O_2 in reaction mixture after complete oxidation of Fc was carried out using time dependent UV-vis spectrophotometric measurements. In 2 mM oxidized solution of Fc^+, 0.02 mM ABTS was added and absorbance was collected at 420 nm for 20 mins measuring after every 1 min. In case of 6 mM of H_2O_2 in reaction mixture a clear absorbance increase could be seen, while in case of 3 mM H_2O_2 inside reaction mixture there was no increase in absorbance for 20 mins. This made sure at 3 mM H_2O_2 conc. in Fc solution, the re-oxidation will take place only because of reformation of H_2O_2 due to enzyme cascade reaction. (Fig. S1)

(ii) Testing the formation of H_2O_2 in absence of O_2 was carried out using UV-vis spectrophotometric measurements for (a) a 2 mM solution of Fc and (b) a 0.023 mM solution of ABTS. A reaction mixture comprising of 0.2 mM glucose, 1.25 µM HRP were prepared in 2.5 mL pH 7.6 0.1 M phosphate buffer for each solution and purged with Ar for 3 h. 100 µL of 1.25 µM GOx solution was prepared separately and purged with Ar for 3 h. Both the solutions were mixed at RT and absorbance was measured. For similar concentrations of reaction mixture and GOx, containing dissolved O_2 absorbance was collected without purging with Ar (Fig. S2 a,b).

(iii) Disassembly of hydrogel (400 µL) was tested against presence of excess buffer in the gel by adding 20 µL to 100 µL of buffer and measuring the change in G' (Fig. S10)

(iv) Minimum concentration of HRP and H_2O_2 required for the hydrogels was carried out using 3 different concentrations of enzyme i.e 0.1, 0.5 and 1.0 mM of HRP and three different concentrations i.e, 0.25, 1.0 and 1.5 M of H_2O_2. All the hydrogels used for experiment were 400 µL in volume. (Fig. S11)

(vi) Kinetic modelling

The model was developed and simulated using MATLAB R2020a SIMBIOLOGY Toolbox.[3] The model was developed using Michaelis–Menten equation (eq.1) by splitting the overall cascade reaction into three major steps as described in SI methods (iii) c Michaelis–Menten studies, Fig. S3, S4, S5. Independent Kinetic parameters were first derived using kinetic assay with triplicated results for each type.

The parameter [ENZ] for the enzyme concentrations in different setups was fitted with iterative least square estimations.

$$V_0 = \frac{V_{max} \times [\boldsymbol{S}]}{K_m + [\boldsymbol{S}]} \quad \text{..... (eq. 1)}$$

Where, V_0 = Initial velocity

V_{max} = Maximum velocity
[S] = Substrate concentration 2.5 mM
K_m = Michaelis constant
Reactions in simulation were defined as:

R1= Reaction between GOx and D-glucose to yield GOx[$FADH_2$]
Substrate [S]= D-glucose
Enzyme [ENZ]= 0.1 mM always kept constant
V_{max} and K_m from table S1 from regeneration

R2= Reaction between GOx[$FADH_2$] and Fc+ to yield Fc.
Substrate [S]= [GOx[$FADH_2$]] formed from R1
Enzyme [ENZ]= 0.1 mM always kept constant
V_{max} and K_m from table S1 from reduction
Concentration of Fc^+ was kept as 2mM

R3= Reaction between GOx[$FADH_2$] and O_2 to regenerate H_2O_2.
Substrate [S]= [GOx[$FADH_2$]] formed from R1
Enzyme [ENZ]= 0.1 mM always kept constant
V_{max} and K_m from table S1 from regeneration
Concentration of O_2 was kept constant as ~ 256.6 µmoles / mL

Oxd.2= Reaction between HRP and Fc in the presence of regenerated H_2O_2.
Substrate [S]= [H_2O_2] from R3
Enzyme [ENZ]= 0.1 mM always kept constant
V_{max} and K_m from table S1 from oxidation
Concentration of Fc was carried on from R2

For all three steps of simulation namely, R1, R2, R3 and Oxd. 2 kinetic coefficients required were obtained from independent MM analysis and have been listed in Table S1.

(vii) Preparation of host and guest polymers:
Amine derivatives of host and guest molecules i.e mono-6-amino-6-deoxy β-cyclodextrin amine[1] (β-$CDNH_2$) and ferrocenecarboxyethylenediamine[2] ($FcCONH_2$) were synthesized for conjugation to polymer chain pAA via peptide coupling. PyBOP as coupling agent in the presence of mild base triethylamine (ET_3N) was utilized for targeting the carboxyl groups on the polymer chain.[2] The synthesis is briefly discussed as follows:

(a) Host polymer
Mono-6-amino-6-deoxy β-cyclodextrin amine (β-$CDNH_2$): β-$CDNH_2$ was synthesized following three step modification starting with β-CD.

β-CD tosylate (β-CD Tos):
β-CD was first converted into a more reactive form β-CD Tos by preparing mixture of (1 molar eq.) β CD with (1.5 molar eq.) 1-(p-Toluenesulfonyl)imidazole in Milli-Q water. After stirring for 4 h at room temperature, 20% wt/vol. NaOH was added to reaction mixture using a pressure equalizing funnel followed by addition of (0.1 molar eq.) NH_4Cl. The reaction was continued overnight. Precipitates were collected and washed twice with cold Milli-Q water and acetone each. Product was dried overnight and analyzed. Yield: 75%.
^{1}H NMR (300 MHz, DMSO-d_6): δ 7.72 (d, J = 8.4 Hz, 2H), 7.39 (d, J = 8.4 Hz, 2H), 5.55–5.89 (m, 14H), 4.75–4.81 (m, 7H), 4.15–4.59 (m, 6H), 3.45–3.72 (m, 28H), 3.10–3.47 (m, 14H), 2.40 (s, 3H).
^{13}C NMR (101 MHz, DMSO-d_6): δ 145.3, 133.0, 130.2, 128.0, 102.1, 82.0, 81.2, 73.5, 73.2, 72.9, 72.3, 70.2, 69.5, 60.3, 21.5
ESI-MS (m/z): calculated for $C_{49}H_{76}O_{37}S$, 1288.4 and found 1311.49 for $[M+Na]^+$.

β-CD azide (β-CDN_3):
β-CD Tos (1eq) and NaN_3 (1eq) were added to 10eq. Milli-Q water and refluxed overnight. After reaction completion 95% water was removed under reduced pressure. (1 molar eq.) 1,1,2,2-tetrachloroethane was added dropwise and mixture was stirred for 30 min. The resultant complex was centrifuged at 5000 rpm at 10℃ for 10 min. Excess water was removed and residue organic layer was collected. Organic solvent was removed under reduced pressure and product was recrystallized using hot water. The recrystallized product was dried overnight and analyzed. Yield: 80%.
^{1}H NMR (300 MHz, DMSO-d_6): δ 5.55–5.89 (m, 14H), 4.75–4.81 (m, 7H), 4.15–4.59 (m, 6H), 3.45–3.72 (m, 28H), 3.10–3.47 (m, 14H), 2.40 (s, 3H).
^{13}C NMR (101 MHz, DMSO-d_6): δ 128.13,125.55, 101.97, 82.0, 81.56, 73.5, 73.2, 72.9, 72.3, 59.94
ESI-MS (m/z): calculated for $C_{42}H_{69}O_{39}N_3$, 1160.0 and found 1160.3 for $[M]^+$

Mono-6-amino-6-deoxy β-cyclodextrin amine (β-CDNH$_2$):

Reduction of β-CDN$_3$ (1 molar eq.) was performed using PPH$_3$ (1.5 molar eq.) after dissolving the in minimum amount of DMF. The reaction mixture was stirred for 1 h at 40℃ after which 0.5 molar eq. NH$_3$ (aq) was added with continued stirring for 1 h. 2.5mL Milli-Q water was added to the reaction mixture and temperature was raised to 90℃ with continuous stirring for 3 h. The reaction was stopped and brought to room temperature. The product was precipitated down using excess acetone. The product was washed for 5-6 times with excess acetone. β-CDNH$_2$ was dried overnight and analyzed. Yield: 65%.

^{1}H NMR (300 MHz, DMSO-d$_6$): δ 5.89–5.63 (m, 14H), 4.92–4.85 (m, 7H), 4.53–4.45 (m, 6H), 3.69–3.54 (m, 28H), 3.46–3.24 (m, 16H).

^{13}C NMR (101 MHz, DMSO-d$_6$): δ 101.97, 82.9, 81.59, 81.5, 73.0, 72.3, 72.1, 59.9

ESI-MS (m/z): calculated for $C_{42}H_{71}O_{39}N$, 1134.3 and found 1134.5 for $[M+H]^+$

Host polymer synthesis (pAA-CD):

Synthesis was performed as stated in Nakahata et al[2] with slight modifications. pAA (1 molar eq.) was dissolved in dry DMF followed by addition of PyBOP (0.06 molar eq.) and ET$_3$N (0.06 molar eq.) with continuous stirring at room temperature. After 2 h of stirring β-CDNH$_2$ (0.1 molar eq.) was added and reaction was stirred for 18 h. The reaction was stopped and modified polymer was precipitated down using excess acetone. The precipitates were collected after centrifuging at 5000 rpm at 15℃ as white residue. The modified polymer was dissolved in Milli-Q water overnight and dialyzed against water (with frequent change) for 6 d using 10 kDa MWCO dialysis tube. The dialyzed polymer solution was freeze dried and analyzed.

^{1}H NMR (500 MHz, D$_2$O): δ 1.6–2.2 (CH$_2$ (pAA)), 2.31–2.65 (CH (pAA)), 3.7–3.90 ($C_{2,4}$ H (β-CD)), 4.00–4.25 ($C_{3,5,6}$ H (β-CD)), 5.15–5.25 (C_1 H (β-CD)).

After analysis 4 % side chain conjugation was found on pAA for β-CD (Fig. S14).

(b) Guest polymer (pAA-Fc):

Ferrocenecarboxyethylenediamine: The synthesis has been reported in Nakahata.et al[2]

Guest polymer synthesis (pAA Fc):

To a solution of pAA (1 molar eq.) in dry DMF and PyBOP (0.06 molar eq.) and ET$_3$N (0.06 molar eq.) was added and stirred for 30 min. FcCONH$_2$ (0.01 molar eq.) was dissolved in DMF and added to pAA solution dropwise at room temperature. The reaction mixture was stirred for 18 h followed by dilution with water. The product was dialyzed against water for 6 days using 10 kDa MWCO dialysis tube. After dialysis the polymer was freeze dried and stored under argon.

^{1}H NMR (500 MHz, D$_2$O): δ 1.60–2.2 (CH$_2$ (pAA)), 2.31–2.650 (CH (pAA)), 4.4 (s, Cp), 4.61 (s, Cp), 4.91 (s, Cp).

After analysis 3 % side chain conjugation was found on pAA for ferrocene (Fig. S15).

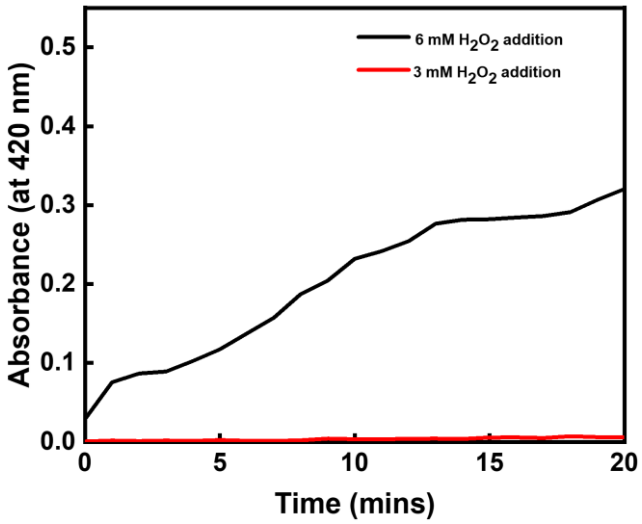

Figure S1. UV-vis spectrophotometric control experiment to test if excess H_2O_2 was present after complete oxidation of Fc which can restart re-oxidation in the CRN. To an oxidized solution of 2 mM Fc^+, 0.02 mM ABTS was added such that in case of excess H_2O_2 present absorption of $ABTS^{+\cdot}$ at 420 nm would be seen. At 3 mM addition of H_2O_2 there is not enough H_2O_2 to react with ABTS or start re-oxidation of Fc in the CRN (red curve), whereas at 6 mM H_2O_2 addition the formation of $ABTS^{+\cdot}$ takes place rapidly (black curve).

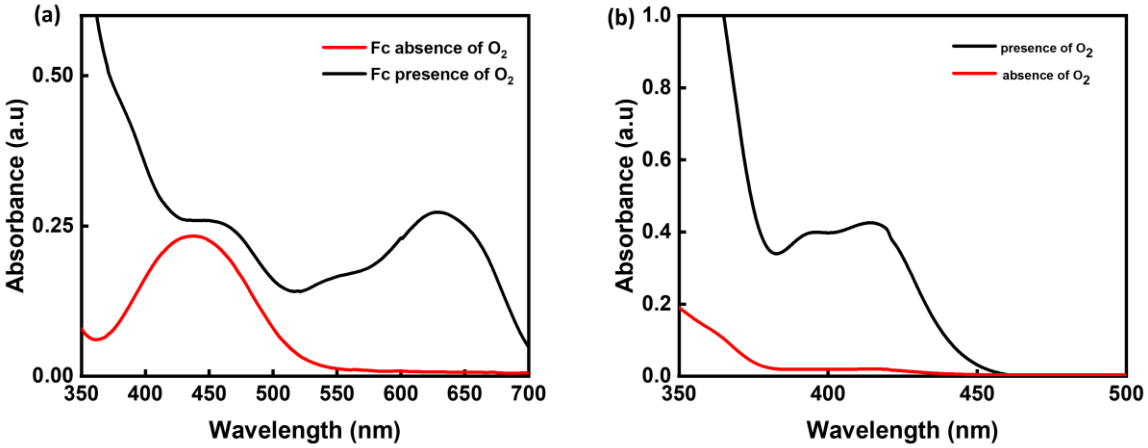

Figure S2. UV-vis spectrophotometric measurements to understand the importance of O_2 for formation of H_2O_2 in the CRN. (a) A 2 mM solution of Fc, 1.25 µM HRP and 0.2 mM D-glucose in 2.5 mL pH 7.6 phosphate buffer was purged with Ar for 3 h to remove O_2. UV-vis measurement was carried out after addition of 1.25 µM GOx into the above solution such that no Fc^+ formed (red curve). At the same point to a similar Fc solution containing both enzymes and D-glucose but without purging with Ar, formation of Fc was seen at 630 nm (black curve). (b) A solution of 1.25 µM HRP, 0.2 mM D-glucose and 0.02 mM ABTS in 2.5 mL pH 7.6 phosphate buffer was purged with Ar for 3 h to remove O_2. Separately a solution of 1.25 µM GOx was purged with Ar for 3 h. UV-vis measurement was carried out after addition of GOx into the above solution. According to UV-vis, no $ABTS^{+\cdot}$ formed (red curve). However, if the solutions were not purged with Ar, instant formation of $ABTS^{+\cdot}$ at 420 nm was observed (black curve).

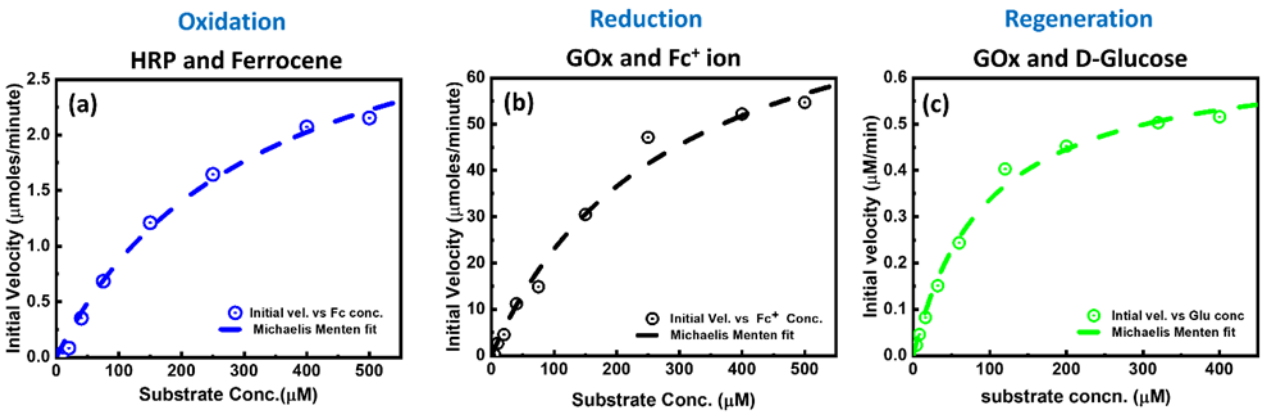

Figure S3. The Michaelis Menten kinetic studies to analyze important kinetic parameters Vmax, Km, Kcat for three different biochemical reactions orchestrating together a negative feedback mechanism inside the system. (a) Represents the oxidation of Fc to Fc^+ ions in the presence of oxidation fuel. (b) Represents reduction of Fc^+ ions back to Fc. (c) Represents autonomous generation of oxidation fuel due to presence of Glucose. The values so obtained (Table S1) were utilized in running simulations based on above experiments to understand the in situ kinetics.

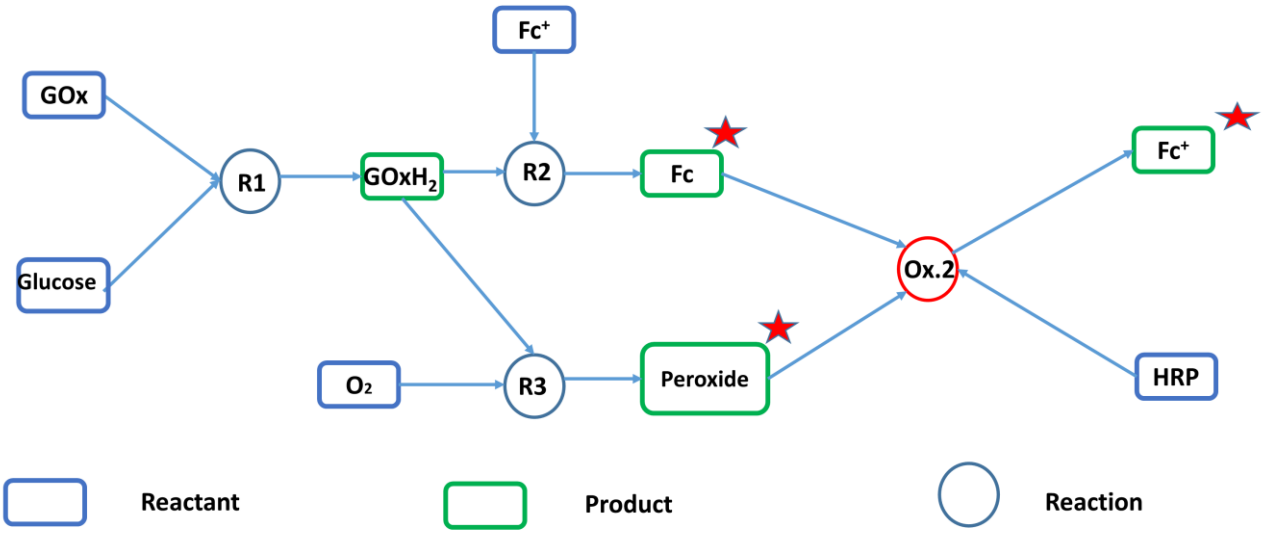

Figure S4. The simulation model set up was based on Michaelis-Menten equations for every part of the cascade reaction network. The model was built in the MATLAB R2020a Simbiology Toolbox[3]. The network was broadly divided into 4 parts namely R1, R2, R3 and Oxd 2. as shown in Fig. S3. R1 originates from reaction between Glucose and GOx forming GOx[$FADH_2$] which was open to react with either Fc^+ ions or atmospheric O_2 to give reactions R2 and R3 respectively. The concentrations of each substrates were maintained equivalent to that found in UV-vis experiments as stated above. After GOx[$FADH_2$] choses either to undergo either R2 or R3 based on independent kinetic parameters obtained from MM kinetic studies, Ox.2 was initiated to see the final outcome of all reactions run in tandem. The products formed independently in reaction R2 and R3 would then react with HRP and regenerate Fc^+ ions.

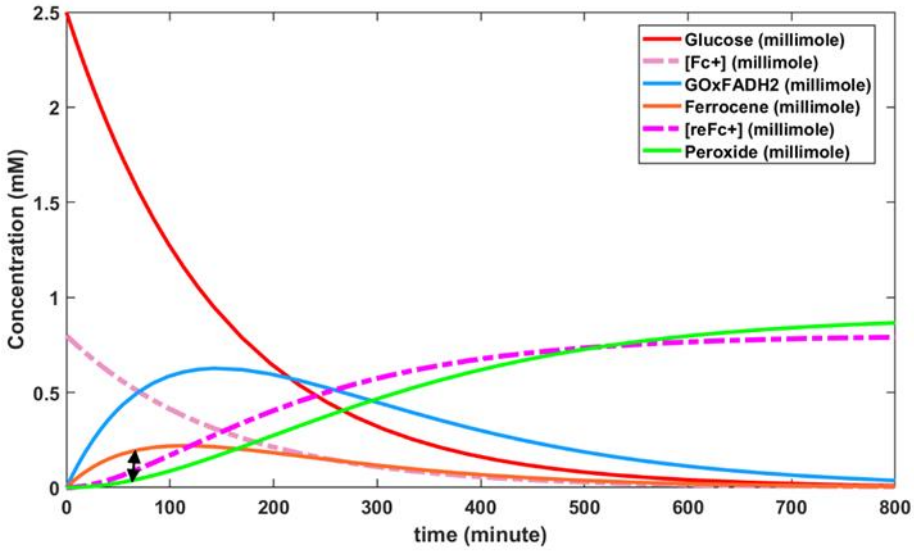

Figure S5. Simbiology Simulation studies obtained after running the model, with all reactions R1, R2, R3 and OX.2 active (Fig S4) demonstrating the role of D-glucose in the fuel driven supramolecular hydrogel. Although D-glucose could be seen simply used up with time, it generated GOx[$FADH_2$] which was the driving factor for all the reactions. The system was able to choose between one of the two available substrates Fc^+ ions and O_2 and create its reaction order. As observed from simulations Fc+ is reduced first leading to increase in concentration of Fc in the system. Only after Fc formation has reached at its highest regeneration of H_2O_2 is initiated in situ. The black double arrow signifies the condition when both Fc and H_2O_2 are regenerated in the system and are available again to initiate re-oxidation hence limiting the induction period.

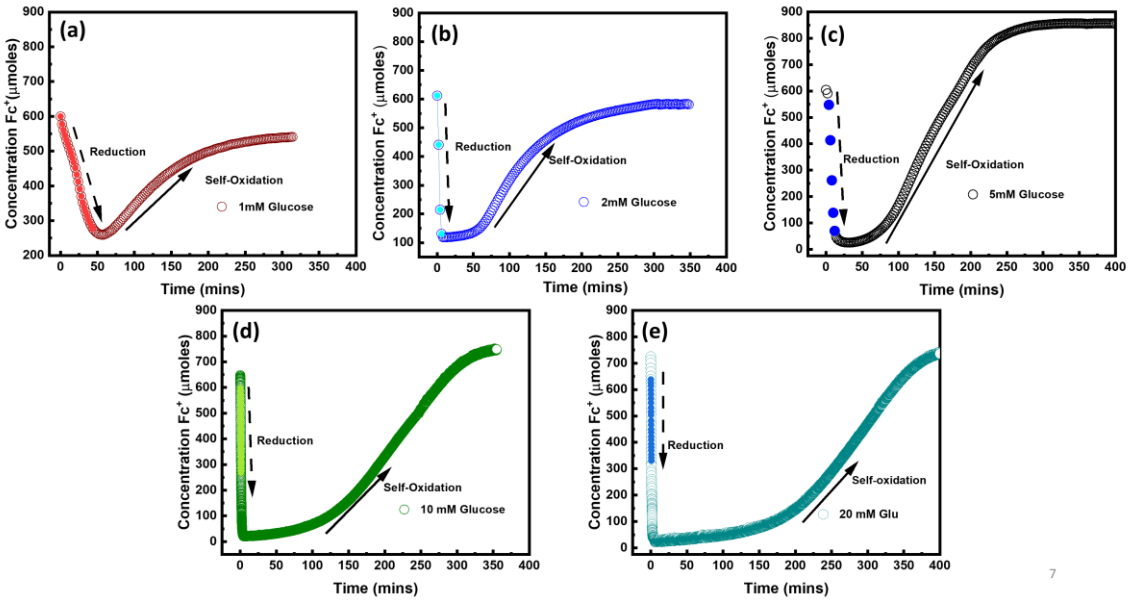

Figure S6. Re-oxidation observed in Ferrocene with different concentrations (1 mM to 20 mM) of D-glucose in the reaction mixture. Each experiment involved two reactions highlighted in each case (i) reduction to Fc (ii) re-oxidation back to Fc^+ ions. The increase in conc. can be seen from (a) to (e) while maintain the consistency in reaction mixture (2mM Fc^+ ions, 0.1 mM HRP and GOx) for each set. While (a) and (b) presented incomplete reduction and re-oxidation due to lack of D-glucose, (c) presented as the model system where the rate of reduction and re-oxidation were highest with shortest induction time period. (d) and (e) presented the case where visible substrate inhibition effects due to very high D-glucose conc. started delaying the negative feedback response.

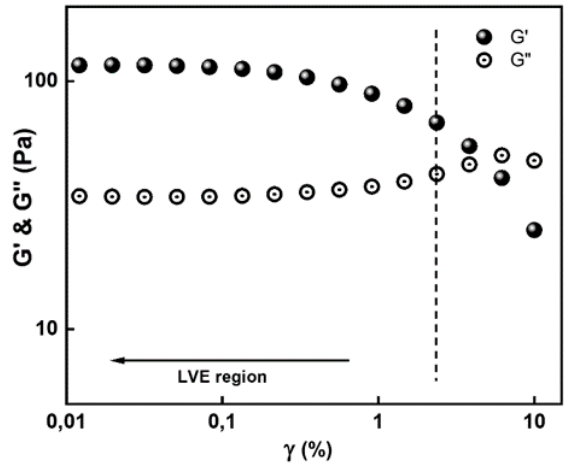

Figure S7. Amplitude sweep for the present hydrogel to determine the linear viscoelastic region (LVE) of the hydrogel. The rheological measurement was conducted at constant ω=1.0 rad/sec with increasing sheer strain γ from 0.01 to 10 %. Deformation of gel was observed after passing γ=1 % with G' reducing to ~30 Pa and G" overlapping at γ=5 %. The region from γ=1 % to γ= 0.01 % was regarded as LVE.

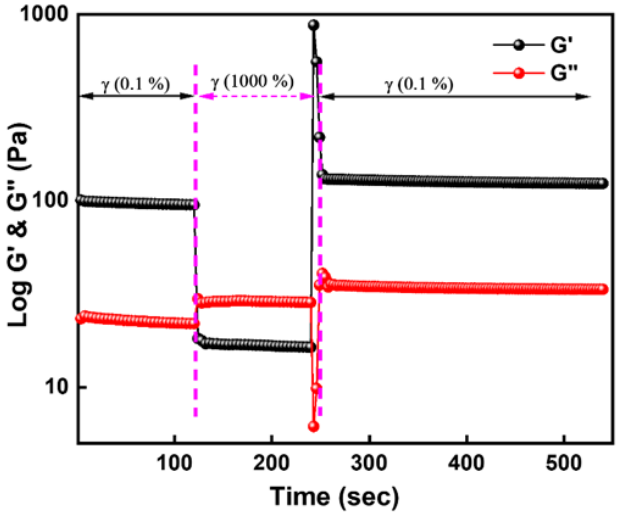

Figure S8. 3 interval thixotropy test (3ITT) to show the self-healing behavior of the supramolecular hydrogel. The first interval consisted of low sheer strain of 0.1 % for 110 seconds to establish storage modulus of the gel G' as 100 Pa. The γ was increased to 1000 % in the second interval leading to disassembly of physical crosslinks in the system transforming the gel into a sol of low viscosity with G' dropping to 25 Pa. The third interval ended with low sheer phase to allow the crosslinks to form again and return the gel to its original stiffness G' 120 Pa.

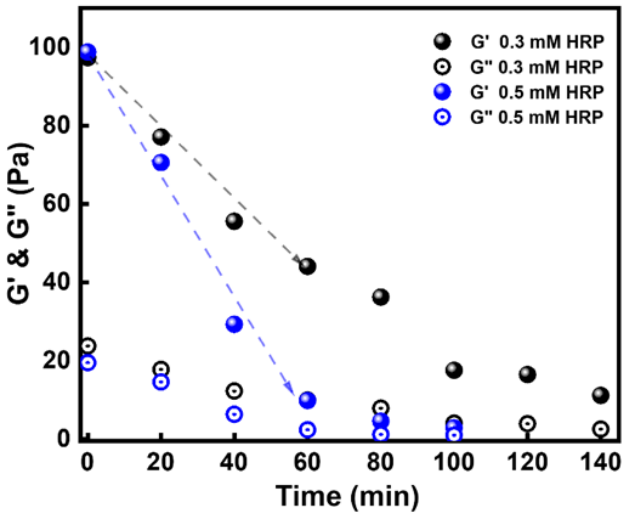

Figure S9. Time dependent gel to sol transition measured using different concentrations of oxidation enzyme HRP (constant 0.01 mM H_2O_2 conc.). The time required for oxidation to sol was highly sensitive to amount of HRP present as decreasing the conc. from 0.5 mM to 0.3 mM increased the time period by nearly half. The arrows indicate the difference in initial velocities of oxidation, as for 0.5 mM HRP conc. at 40 min the G' had reduced to 36 Pa, while the later arrived at this value only after 80 min of oxidation.

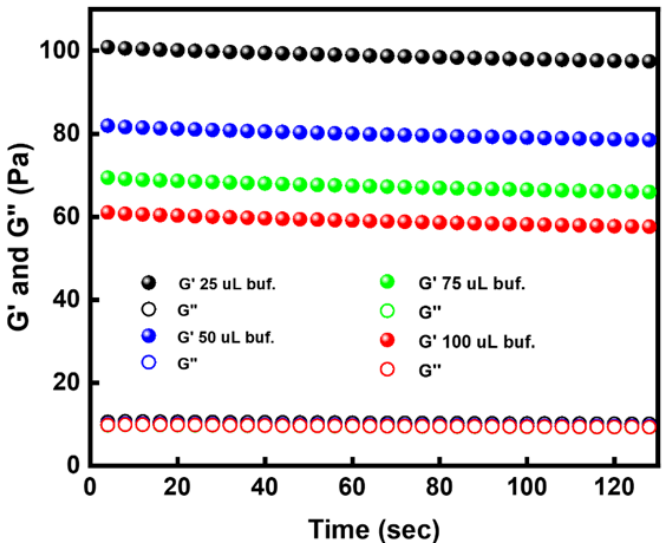

Figure S10. Effect of dilution on control hydrogel (400 µL) was analyzed by addition of different volumes (25 µL to 100 µL) of phosphate buffer (pH 7.0, 0.1 mM). The resulting hydrogel was equilibrated for nearly 3 h (same period required for oxidation) and final G' was measured. It could be observed that the hydrogel does not transform into sol even on 25% dilution on addition of 100 µL excess buffer.

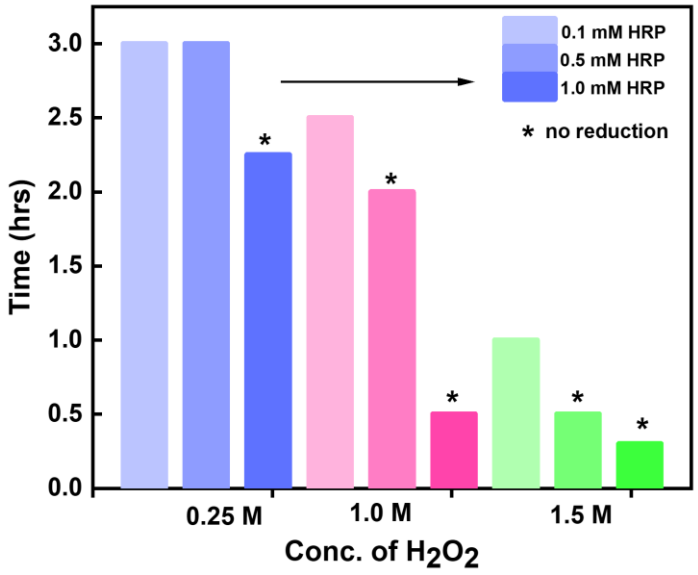

Figure S11. Control studies to define the minimum concentration of HRP and H_2O_2 required for oxidation of gels. The hydrogels used for all studies were Time required for sol formation on addition of different concentration of HRP (0.1, 0.5, 1.0 mM) with 0.25, 1.0 and 1.5 M addition of H_2O_2 substrate. The time required for transformation decreased with increase in concentration of H_2O_2 supplied, although the probability of same sol reassembling back to gel declined at these higher concentrations as marked by an (*) sign. Hence, a minimum concentration of H_2O_2 0.25 M was chosen to be added to hydrogels.

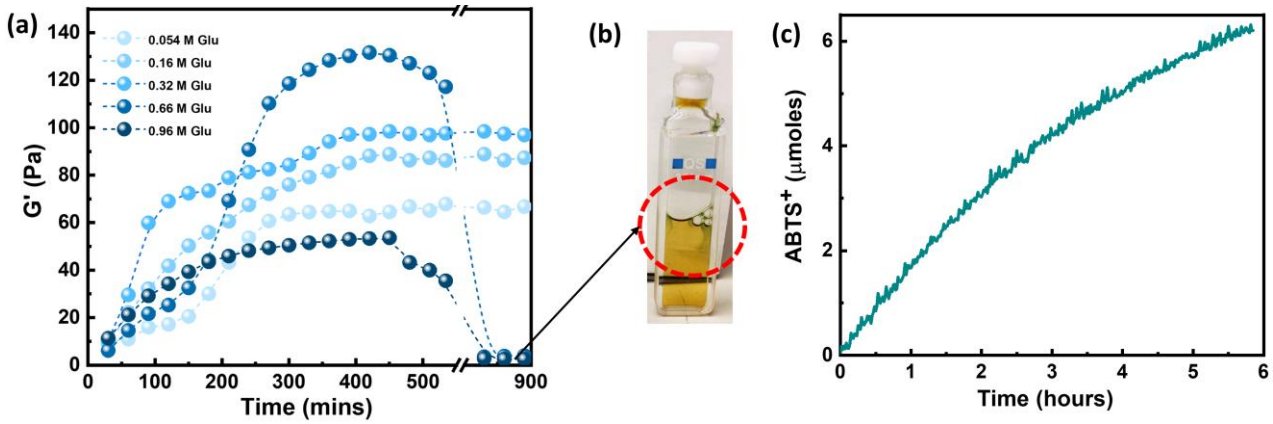

Figure S12. (a) re-oxidation leading to sol formation at the end of reduction experiments in hydrogels was verified by addition of chromophore substrate ABTS to the sol collected at the end of each experiment in case of 0.66 M & 0.96 M conc. of glucose. (b) Visible appearance of blue color ($ABTS^{\cdot+}$) was seen instantly after addition of ABTS to the sol. (c) Time dependent UV-vis spectroscopy measurement was conducted at 420 nm to observe continuous formation of hydrogen peroxide in the system.

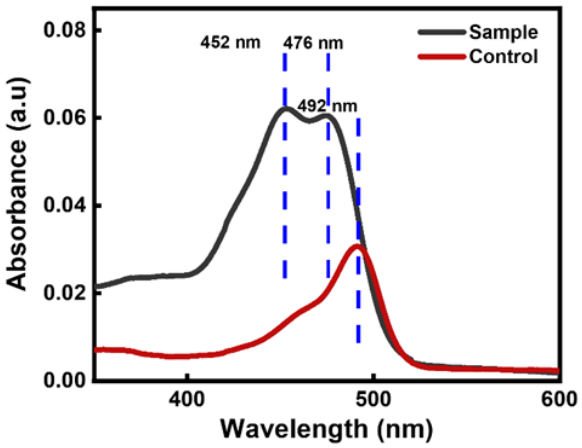

Figure S13. A visible blue shift in absorbance of dye in the case of glucose sensor hydrogel was observed in comparison to the control hydrogel. This blue shift was perceived due to presence of H_2O_2 regenerated in the system leading to oxidation of dye.

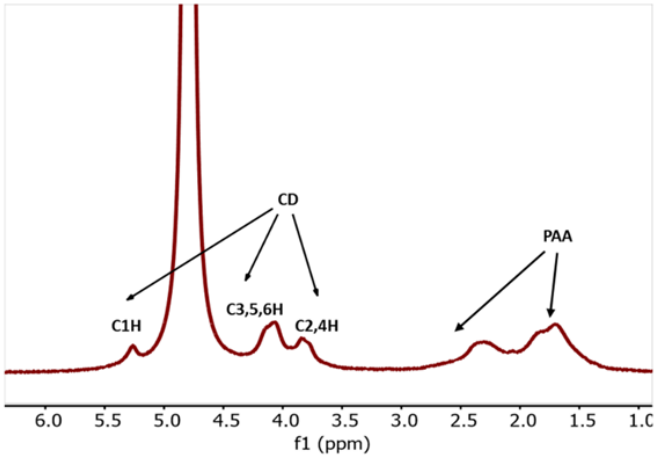

Figure S14. ^{1}H NMR (500 MHz, D_2O at 30℃) for pAA-CD. Side chain substitution for β-$CDNH_2$ was calculated as ~ 4%.

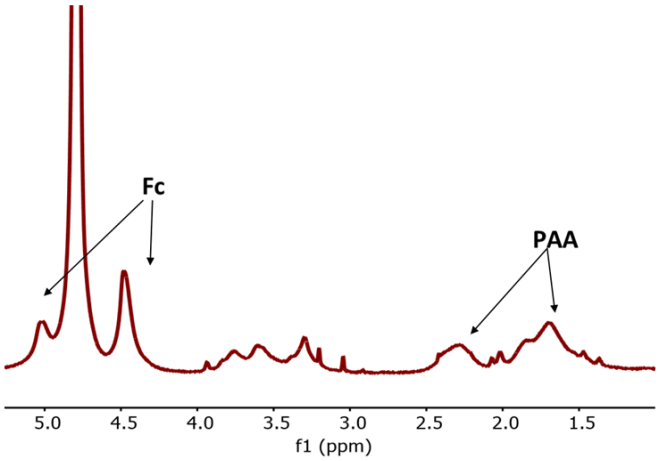

Figure S15. 1H NMR (500 MHz, D2O at 30℃) for pAA-Fc. Side chain substitution for $FcCONH_2$ was calculated as ~ 3%.

Table S1. Enzymatic parameters obtained from Michaelis–Menten kinetic fits to the enzymatic assay data shown in Fig. S3

	Oxidation[a]	Reduction[b]	Regeneration[c]
Vmax (μM/min)	3.65	88.90	0.6559
Km (μM)	321.95	286.42	94.529
Kcat (1/min)	3,215.86	1,42240.0	10,494.7
Kcat/Km	9.98	496.613	110.556

[a] Fc as substrate. [b] Fc^+ as substrate. [c] D-glucose as substrate

References

[1] W. Tang, S.-C. Ng, *Nat.Protoc.* **2007**, *2*, 3195-3200.
[2] M. Nakahata, Y. Takashima, H. Yamaguchi, A. Harada, *Nat. Commun.***2011**, *2*, 511.
[3] S. Milker, M. J. Fink, N. Oberleitner, A. K. Ressmann, U. T. Bornscheuer, M. D. Mihovilovic, F. Rudroff, *ChemCatChem* **2017**, *9*, 3420-3427.